Poly(styrene-*b*-vinylphenyldimethylsilanol) and Its Blends with Homopolymers

Yu-Kai Han, Eli M. Pearce,* and T. K. Kwei*

Department of Chemical Engineering, Chemistry, and Materials Science, Polytechnic University, Brooklyn, New York 11201

Received June 1, 1999; Revised Manuscript Received November 9, 1999

ABSTRACT: Block copolymers of vinylphenyldimethylsilanol (VPDMS) and styrene were synthesized by living anionic polymerization of vinylphenyldimethylsilane and styrene with *sec*-butyllithium as initiator in THF at −78 °C, followed by an oxygen insertion reaction via oxyfunctionalization, in part or all, with dimethyldioxirane. The resulting silanol group (≡Si−OH) at the 4-position of the styrene copolymer acts as a hydrogen bond donor, thus enhancing miscibility with polymers containing hydrogen bond accepting groups. The block copolymers containing varying amounts of silanol groups and their blends with poly(*n*-butylmethylmethylacrylate) (PBMA), poly(vinylpyrrolidone) (PVPr), and poly(vinylpyridine) (P4VPy) were characterized by temperature modulated differential scanning calorimetry (MDSC) and Fourier transform infrared spectroscopy (FTIR). In blends with PBMA, the PVPDMS block is miscible with PBMA when it contains about 11−33% silanol groups, and the polystyrene blocks retain their identity as separate domains. These observations suggest microphase separation as the dominant mechanism. However, at higher silanol contents, the T_g results indicate the presence of three different domains and are indicative of a microphase−macrophase separation mechanism. The block copolymer containing 21% VPDMS units, PVPDMS-21, forms transparent films when blended with PVPr at all ratios; again, the PS blocks are unaffected, and the T_g results conform to the predictions of a microphase separation mechanism. There is also a positive deviation of the T_g of the mixed phase from the calculated weight-average value as a result of strong hydrogen bonding between the silanol and amide carbonyl groups. The interaction between pyridine and silanol group results in a large shift in the −OH stretching frequency ($\Delta\nu = 223$ cm^{-1}), indicative of strong intermolecular hydrogen bonding interaction which is evidenced also by the presence of the pyridinium structure in the FTIR spectra. The strong interaction is responsible for microphase separation as the dominant mechanism in morphological development with a large synergistic T_g effect. On the basis of spectroscopic and T_g results, the relative strength of intermolecular hydrogen bonding in the blends can be ranked in the order P4VPy > PVPr > PBMA. The strength of the intermolecular hydrogen bonding between the homopolymer and the silanol containing block, in relation to the self-association of silanol groups, governs the mechanisms of morphological development, i.e., microphase separation versus microphase−macrophase separation.

Introduction

The microphase vs macrophase relationships in the blends of a diblock copolymer AB with a homopolymer C have been analyzed and compared with morphological observation in a number of publications, including a recent paper by Hellmann et al.[1] In their analysis, calculations were carried out for blends in which the homopolymer C is immiscible with the A block but interacts favorably (negative interaction parameter ξ) with the B block. The most important parameter that governs phase separation from a homogeneous state is the magnitude of the interaction parameter ξ. The conditions that favor microphase separation (A phase plus a mixed B + C phase), macrophase separation (C phase plus a mixed A + B phase), and microphase−macrophase separation (a macrophase of C plus microphases of A and B) were elucidated. To test these predictions, we have synthesized earlier[2] a diblock copolymer comprised of polystyrene and poly(*p*-hydroxystyrene). Three homopolymers were chosen for blending studies, namely, poly(*n*-butylacrylate), poly(ethylene oxide), and poly(4-vinylpyridine), each of which is immiscible with polystyrene, PS, but is miscible with poly(4-hydroxystyrene), PHOST. The nature of intermolecular interaction between the PHOST block and the homopolymers was studied by infrared spectroscopy, and the relative strengths of interaction in the three blends were deduced from the shift in the hydroxyl stretching frequency of the phenol group. The phase relationships in the three blends were studied by glass transition temperature measurements, and the results are in full agreement with theoretical predictions. We have now extended our investigation to a series of diblock copolymers, poly(styrene-*b*-vinylphenyldimethylsilanol), in which the silanol content of the second block varying from 11 to 100% provides us with an additional avenue to probe phase separation behavior. The homopolymers selected for the present study are poly(butylmethyl acrylate) (PBMA), poly(vinylpyrrolidone) (PVPr), and poly(4-vinylpyridine) (P4VPy), all of which are immiscible with PS but miscible with poly(vinylphenyldimethylsilanol), PVPDMS.[3−8] Again, infrared spectroscopy and T_g measurements were the major tools used; the results are reported herein.

Experimental Section

Materials. All chemicals were purchased from Aldrich and Gelest Inc. and purified before use according to standard procedures.[9] Poly(*n*-butyl methacrylate) (PBMA, poly(vinylpyridine) (P4VPy), and poly(*n*-vinylpyrrolidone) (PVPr) with reported molecular weights (M_w) of 50 000, 40 000, and 30,000, respectively, were purchased from Aldrich Inc. They were dried under vacuum at 60 °C for 48 h before use. The T_g values of the three polymers were 33, 147, and 174 °C, respectively.

Characterizations. GPC. Gel permeation chromatography (GPC) was carried out with a Waters analytical GPC system

10.1021/ma990852n CCC: $19.00
Published on Web 01/27/2000

Scheme 1. Synthesis of 4-Vinylphenyldimethylsilane

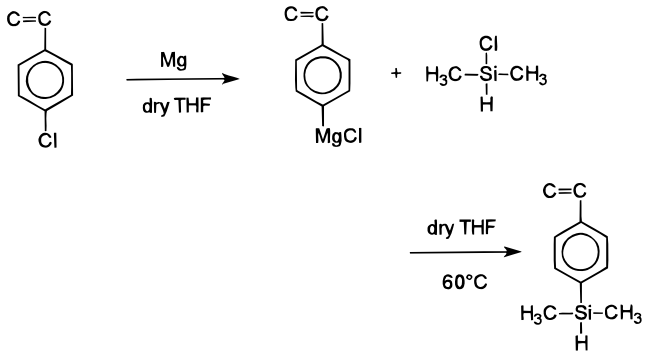

(model 510 included HPLC pump (U6K)), equipped with a sample injector, a differential refractometer (410), and a set of three columns (phenol gel, Phenomenex Inc.) of sizes 103, 104, and 105 Å. The GPC instrument was calibrated with monodisperse polystyrene standards before use. The measurements were carried out at 35 °C with THF as the elution solvent, and the flow rate was 1.00 mL/min. The concentrations of the samples were 0.1 wt % in all cases. The molecular weight values reported herein are PS equivalents.

NMR. ^{1}H NMR spectra were recorded with a Varian EM 390 90 MHz instrument. Deuterated acetone and chloroform were used as solvents.

TGA. Thermogravimetric analysis (TGA) was performed with a Dupont 2100 TGA instrument at a heating rate of 20 °C/min under nitrogen (flow rate 40 mL/min).

TMDSC. Glass transition temperatures were determined using a TA 2920 thermal analyzer equipped with a temperature modulated differential scanning calorimeter (TMDSC). The measurements were carried out under N_2 at a heating rate of 5 °C/min, with a temperature oscillation of ±1 °C/min. Experiments were carried out in the reversing heat flow mode. The sample size was about 6−10 mg. Each sample was first scanned from a low initial temperature to 100 °C, maintained at that temperature for 0.5 min, quenched to the initial temperature, and scanned again. The T_g's were taken as the onset points of the specific heat jumps observed in the second scans.

Fourier Transfer Infrared Spectrometry (FT-IR). A Perkin-Elmer 1600 series FT-IR spectrometer was used to study shifts in the hydroxyl stretching frequency as a measure of the inter- or intramolecular hydrogen bonding interaction in polymers. The measurements were carried out under a N_2 atmosphere. Thirty-two scans were collected and signal averaged at a resolution of 4 cm^{-1}.

Synthesis of 4-Vinylphenyldimethylsilane (Monomer). 4-Vinylphenyldimethylsilane was synthesized according to the methods described in the literature[3,10−12] (Scheme 1).

Magnesium turnings (10 g, 0.22 mol) were mixed with dry THF (25 mL) in a round-bottom flask equipped with a condenser and nitrogen inlet. About 5 mL of 4-chlorostyrene (0.2 mol) in dry THF (25 mL) and 1 mL of 1,2-dibromoethane were added into the round-bottom flask. The reaction mixture was kept under refluxing condition, and the remaining 4-chlorostyrene solution in THF was added dropwise to prevent too vigorous a reaction. The reaction was allowed to proceed for more than 1 h and then was cooled to room temperature. Dimethylchlorosilane (0.2 mol) in dry THF (20 mL) was added dropwise through a syringe, and the reaction was allowed to proceed for an additional 2 h. The reaction mixture was filtered, extracted with ether, and distilled under reduced pressure. 4-Vinylphenyldimethylsilane was purified further by fractional distillation at 50 °C (0.1 mmHg, yield 75%) [lit.[2] 61 °C (0.3 mmHg)] of a colorless liquid. ^{1}H NMR (90 Hz, CCl_4): δ 7.2−7.6 (4H, m, phenyl), δ 6.5−6.9 (1H, 2d, vinyl CH) δ 5.2−5.8 (2H, 2d, vinyl CH_2), δ 4.4−4.7(1 H, m, Si−H), δ 0.2−0.4 (6H, d, $SiCH_3$). IR: 2117 cm^{-1} (Si−H), 1269 cm^{-1} (=CH_2), 1600 cm^{-1} (phenyl), 1389 and 1108 cm^{-1} (Si−phenyl), 1252 and 883 cm^{-1} (Si−CH_3).

Synthesis of the Block Copolymer of 4-Vinylphenyldimethylsilane and Styrene. Styrene was washed with 5% NaOH, dried over $MgSO_4$, and distilled over calcium hydride (CaH_2) under a nitrogen atmosphere. Both styrene and 4-vinylphenyldimethylsilane were then distilled twice over benzylmagnesium chloride (10 mL, 0.5 M solution in THF) at 0 °C under argon atmosphere and stored at 0 °C. Dried THF was first degassed and distilled into a round-bottom flask equipped with a high-vacuum stopper under liquid nitrogen and then frozen at liquid nitrogen temperature. All the polymerizations were carried out at −78 °C with stirring under high vacuum in an all-glass predried apparatus. Styrene monomer was distilled into the reaction bottle containing dried THF. A specific amount of *sec*-butyllithium (2.0 M in THF solution) was added using a gastight syringe with a built-in valve. The color of the reaction solution was light yellowish. After 30 min, a sample of the reaction solution was removed for molecular weight determination. The second monomer was then distilled into the reaction bottle; the color of the reaction mixture remained unchanged. After 2 h, the reaction solution was terminated by injecting 5 mL of purified methanol. The color of the solution now changed from yellowish to colorless. The polymer was precipitated in methanol and redissolved in acetone twice. The block-copolymer synthesis procedure was described schematically as follows (Scheme 2).

Oxygen-Insertion Reaction. A mixture of distilled water (50 mL), acetone (40 mL), and sodium bicarbonate (24 g) was put into a round-bottom flask equipped with a solid-addition funnel containing potassium peroxomonosulfate (50 g). The air condenser was filled with a mixture of dry ice and 2-propanol and connected to the reaction bottle. The bottom of the dry ice condenser was attached with a receiving flask kept in a dry ice acetone bath. Argon gas was gently passed through the reaction bottle. The dimethyldioxirane solution was collected in a receiving flask and reacted immediately with the block copolymer to desired conversions (Scheme 3). The conversion of Si−H to Si−OH was determined by NMR from the ratio of the peaks at δ 4.4 ppm (Si−H) and δ 4.9−5.1 ppm (Si−OH). The use of acetone as solvent minimizes the self-association of silanol groups and subsequent formation of siloxane linkages. In the ensuing text, the numeral after PVPDMS indicates the percentage of Si−H groups that have been transformed to Si−OH.

Preparation of Films. Films of polymers and blends were cast from acetone solutions (5%). Various compositions were prepared by mixing appropriate amounts of these solutions. Films for DSC measurements were obtained by casting solutions onto an aluminum dish. For FTIR measurements, thin films were cast from solutions onto potassium bromide (KBr) windows at room temperature. Solvents were removed slowly by evaporation at room temperature, and the films were dried under vacuum (10^{-3} mmHg) at 40 °C for 1 h.

Results and Discussion

Poly(ST-*b*-VPDMS-0). The molecular weight distribution measurement of the silane block copolymer from GPC shows that the M_w/M_n is 1.06 for polystyrene, and the polydispersity of the block copolymer of styrene and vinylphenyldimethylsilane is 1.16. The number-average molecular weight of the polystyrene block is 35 000, and that of the block copolymer is 88 000 and (Figure 2). Thus, the two blocks are approximately equal in the number of segments, 337 vs 327. The T_g's of poly(vinylphenyldimethylsilane) (PVPDMS-0) and polystyrene (PS) were determinated to be 105 and 103 °C, respectively. Because of the proximity of the two T_g's, only one glass transition was seen for the block copolymer. It is interesting that although PVPDMS-0 contains a bulky side group, −$SiH(CH_3)_2$, there is no obvious difference in the glass transition temperature between PS and PVPDMS-0.

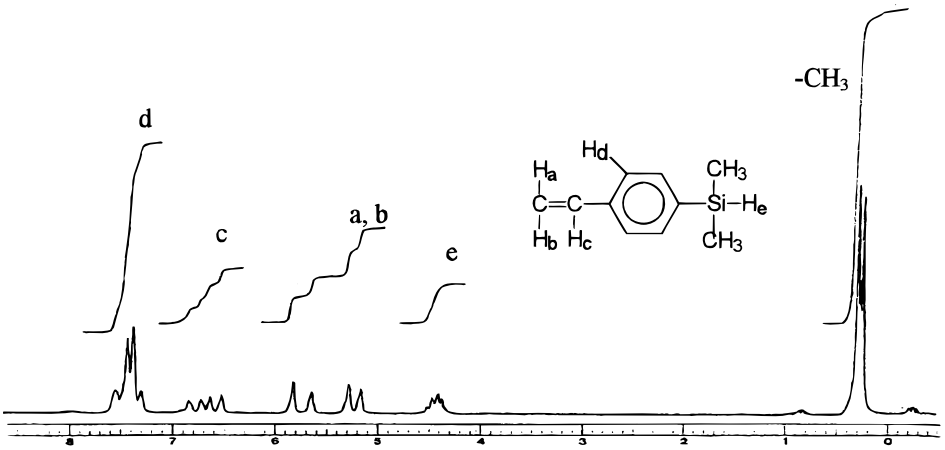

Figure 1. ^{1}H NMR of 4-vinylphenyldimethylsilane.

Scheme 2. Synthesis of Diblock Copolymer

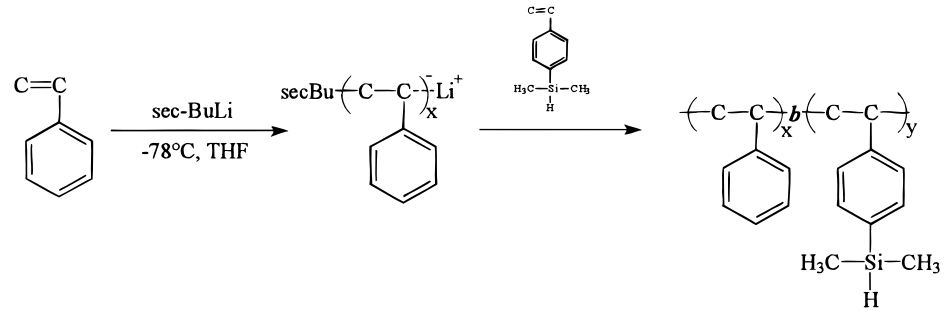

Scheme 3. Oxygen Insertion Reaction of the Block Copolymer

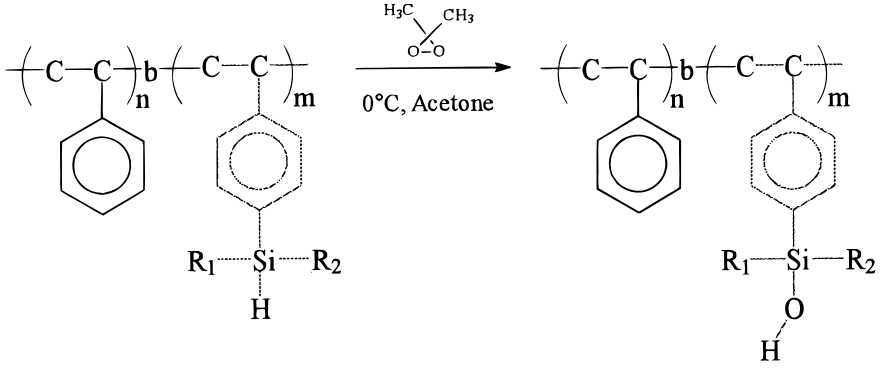

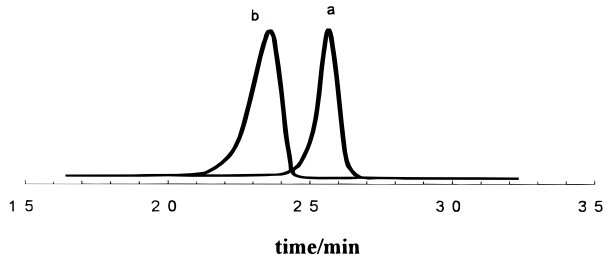

Figure 2. Molecular weight distribution of (a) polystyrene (M_w/M_n) = 1.06 and (b) block copolymer (M_w/M_n) = 1.16, M_n = 88 000.

FTIR. The most important absorption band of PS-*b*-PVPDMS-0 is located at 2117 cm^{-1} which can be assigned to the Si−H stretching mode (Figure 3).

PS-*b*-PVPDMS. When the Si−H groups are converted to Si−OHs, the stretching band at 2117 cm^{-1} decreases in intensity, and two new broad bands appear. The absorption band at 3623 cm^{-1} can be attributed to the free silanol groups, and the absorption in the 3300−3445 cm^{-1} region, to the self-associated silanol groups. The infrared frequency shift ($\Delta\nu$) of silanol stretching bands due to self-association is about 333 cm^{-1}, which can be described as a "medium" type hydrogen bond.[13,14] Similar results were found in previous studies[3−8] using random copolymers. In comparing the frequency shifts due to the self-association of silanol groups in block and random copolymers having the same Si−OH contents, we found that the shifts are smaller for the block copolymers when the silanol contents are low. The silanol groups in the random copolymers have styrene units as their neighbors whereas in the block copolymers they are shielded by intervening vinylphenyldimethylsilane units which are bulkier than styrene and offer more steric hindrance and larger intermolecular screening effect. Consequently, the hydroxyl frequency shifts are smaller.[4−8] Concurrent with the appearance of the broad absorption at 3300−3445 cm^{-1}, a new small broad band at 1040−1100 cm^{-1} emerges and increases in intensity as silanol content increases. This absorption band is attributable to Si−O−Si stretching. Although

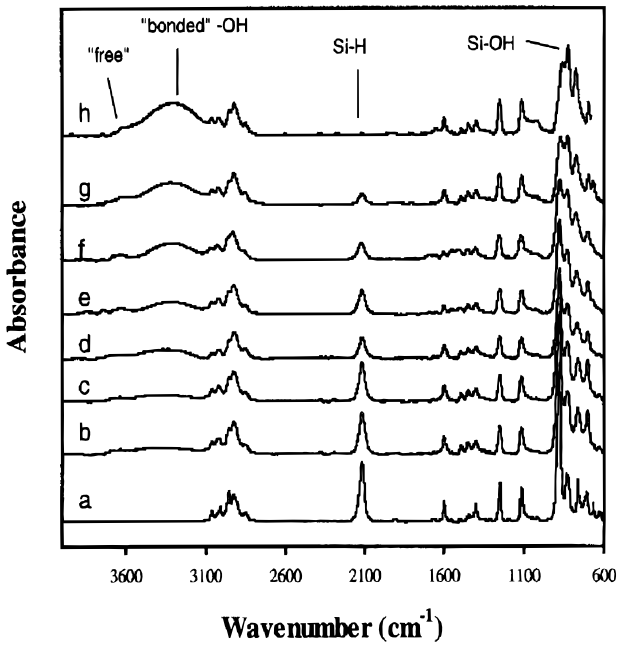

Figure 3. Infrared spectra of (a) pure Poly(ST-*b*-VPDMS-0), (b) PS-*b*-PVPDMS-11, (c) -21, (d) -33, (e) -49, (f) -65, and (g) -82.

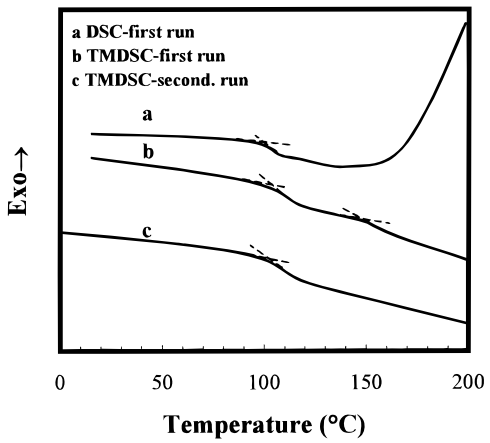

Figure 4. Thermal analysis from (a) DSC, (b) TMDSC reversing heat flow first run, and (c) second run of PS-*b*-PVPDMS-100.

this broad band has been assigned to contain both symmetric and asymmetric components,[16] we were unsuccessful in resolving the two by curve fitting or subtraction methods. The formation of siloxanes in the block copolymers upon heating complicates the T_g measurements and is to be avoided, if at all possible. Accordingly, mild conditions were used for film preparation.

Figure 4 shows the results of the thermal analysis studies. In curve a obtained by conventional DSC, the T_g of the PS block is readily identified at 100 °C, followed by a large exothermic event beginning at 150 °C which obscures other thermal events. The problem was alleviated by the use of TMDSC in the reversing heat flow mode; a distinct T_g was observed at 141 °C. Although there is some uncertainty as to whether this second transition represents the true T_g of the silanol-containing block due to the possibility of siloxane formation during the thermal scan, the error is believed to be small at the heating rate used because there was no sign of weight loss in the TGA curves up to 150 °C.

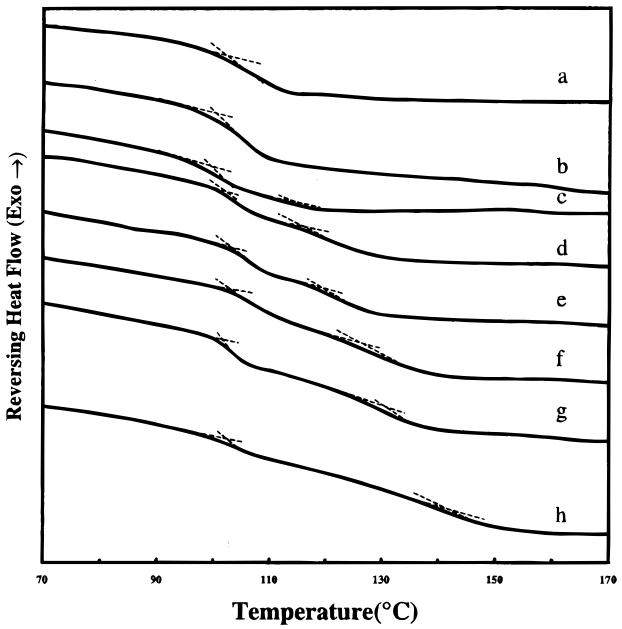

Figure 5. TMDSC reversing heat flow of (a) pure PS-*b*-PVPDMS-0, (b) -11, (c) -21, (d) -33, (e) -49, (f) -65, and (g) -82 conversion.

Table 1. Glass Transition Temperatures of PS-*b*-PVPDMS

code mol % silanol	conversion	PS T_{g1}(°C)	PVPDMS T_{g2}(°C)
PS-*b*-PVPDMS-0	0	102	
PS-*b*-PVPDMS11	11	101	
PS-*b*-PVPDMS21	21	103	114
PS-*b*-PVPDMS33	33	102	116
PS-*b*-PVPDMS49	49	103	119
PS-*b*-PVPDMS65	65	102	127
PS-*b*-PVPDMS82	82	101	131
PS-*b*-PVPDMS-100	100	103	141

However, if the scan continues to 200 °C, the transition was no longer observed in the second scan as a result of extensive cross-linking through siloxane linkages.

Figure 5 shows the T_g's of several block copolymers having different amounts of silanol groups. The glass transition temperatures of the silanol containing block in PVPDMS-11 cannot be observed clearly because the T_g's of the two blocks are too close to each other. As the silanol group content increases, the second T_g becomes identifiable. The results are summarized in Table 1. The second T_g is comparable to that of the random copolymer of styrene and VPDMS having a similar silanol content.[3]

In examination of the glass transition temperatures of poly(styrene-*r*-vinylphenyldimethylsilanol)[26] poly(styrene-*r*-vinylphenylmethylphenylsilanol), and poly(styrene-*r*-vinylphenyldiphenylsilanol),[27] Pearce and coworkers concluded that the glass transition were controlled by two factors, namely, the balance of free volumes or packing densities and self-associated hydrogen-bonding interaction. As we have discussed earlier, the silanol units are separated by different neighbors, vinylphenyldimethylsilanol units in the former and styrene units in the latter. Although the larger silane unit offers better intermolecular screening effect which is unfavorable to hydrogen bonding, it may at the same time promote efficient packing of chains because of the similarity in the sizes of the silanol and silane moieties. Possibly, the two factors compensate each other so that there are very little differences between the T_g's of the random copolymers and block copolymers.

Table 2. Glass Transition Temperatures of PBMA/ PS-*b*-PVPDMS Blends 50/50 (w/w)

blend composition	PS T_{g1}[a] (°C)	PVPDMS T_{g2}[b] (°C)	PBMA T_{g3}[c] (°C)	film acetone
0			33	clear
PS-*b*-PVPMDS-11	99	54 (101)[d]		clear
PS-*b*-PVPMDS-22	101	62 (114)[d]		clear
PS-*b*-PVPMDS-33	99	70 (116)[d]		clear
PS-*b*-PVPMDS-49	100	105 (119)[d]	41	opaque
PS-*b*-PVPMDS-65	102	120 (127)[d]	39	opaque
PS-*b*-PVPMDS-82	101	125 (131)[d]	35	opaque
PS-*b*-PVPMDS-100	102	140 (141)[d]	34	opaque

[a] T_{g1} = glass transition temperature of the PS block. [b] T_{g2} = glass transition temperature of the PVPDMS phase. [c] T_{g3} = glass transition temperature of the PBMA phase. [d] Glass transition temperature of the PVPDMS phase before blending.

Blends of Diblock Copolymer AB with Homopolymer C. We have stated earlier that the most important parameter governing phase separation mechanism is the negative interaction parameter ξ between B and C. The three homopolymers employed in this study have different strengths as hydrogen bond acceptors, in the order PBMA < PVPr < P4VPy.[25] Their blends with poly(styrene-*r*-vinylphenyldimethylsilanol) have already been studied by Lu et al.,[3−8] and the earlier results serve as a useful background for this investigation. Additionally, the relative volume of the homopolymer to the B block is also an important parameter in theoretical calculations. To minimize disparities in the chain volumes, we have chosen the homopolymer to have molecular weights as close as possible to each other and to the B block, namely, 50 000 for PBMA, 40 000 for PVPr, 30 000 for P4VPy, and 53 000 for the B block.

For blends of ST-*b*-VPDMS-11, ST-*b*-VPDMS-21, and ST-*b*-VPDMS-33 with PBMA 50/50 (w/w), the blend solutions and the films were visually clear. Each blend film shows two T_g's, one of which is the same as the T_g of PS and the other between the T_g's of PBMA and the silanol-containing block. Blend films prepared from block copolymers having silanol contents from 49 up to 100% were opaque, and three glass transition temperatures corresponding to those of the component polymers/ blocks were seen in thermal scans. The T_g results are shown in Table 2. For the purpose of comparison, the T_g of the block before blending is given in parentheses.

It is clear from the T_g values in Table 2 that the PS domain is unaffected by PBMA in all cases. The homopolymer is incorporated in the PVPDMS domain when the silanol content is 11, 21, or 33% to cause a lowering of the T_g of the microphase. The behavior is typical of the microphase separation mechanism. In contrast, when the block copolymers contain a higher percentage of silanol groups, from 49% up, the three T_g's, corresponding to the T_g's of PS, PVPDMS, and PBMA, respectively, are consistent with microphase−macrophase separation although the PDPMS microphase may contain some trapped PBMA and the PBMA macrophase may contain some PVPDMS. The opacity of the blend films supports this interpretation. In this regard, blends of poly(styrene-*b*-*p*-hydroxystyrene) with poly(*n*-butyl acylate)[2] have also been reported to undergo microphase−macrophase separation.

The reason that PBMA is not incorporated in the silanol-containing block when the silanol content is 49% or higher can be traced to the strong self-association of the Si−OH groups in the block copolymers. This can be seen in the FTIR spectra shown in Figure 6. The new absorption band at 3522 cm^{-1} in the blends of block

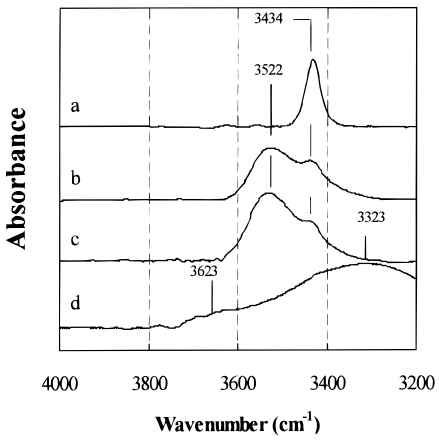

Figure 6. Infrared spectra of −OH stretching region 3200−4000 cm^{-1} for (a) PBMA, (b) PS-*b*-PVPDMS-21, (c) PS-*b*-PVPDMS-33 blend, and (d) PS-*b*-PVPDMS-49 blend 50/50 (w/w).

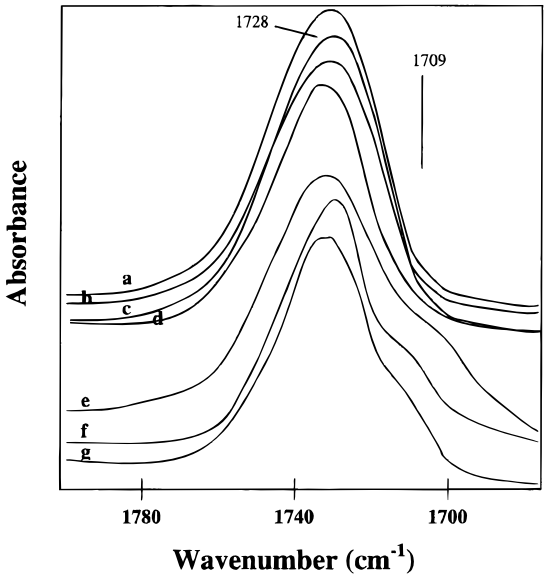

Figure 7. Infrared spectra of carbonyl stretching region 1700−1780 cm^{-1} for PS-*b*-PVPDMS/PBMA 50/50 (w/w) blends: (a) PBMA, (b) PS-*b*-PVPDMS-82, (c) PS-*b*-PVPDMS-65, (d) PS-*b*-PVPDMS-49 (e) PS-*b*-PVPDMS-33, (f) PS-*b*-PVPDMS-21, and (g) PS-*b*-PVPDMS-11.

polymer-21 and -33 is attributable to hydroxyl groups hydrogen bonded to the carbonyl groups of PBMA. However, in the copolymer-49 blend, this peak is not seen; instead, only the broad band at 3223 cm^{-1} due to self-association of hydroxyl groups is prominent. The systematic increase in the intensity of the 3522 cm^{-1} peak with PBMA content in the PVPDMS-49 blends gives support to our assignment. That the frequency shift of 103 cm^{-1} (from that of free Si−OH band) for the silanol−carbonyl interaction is smaller than that for self-association, 223 cm^{-1}, indicates that intermolecular hydrogen bonding is weaker than silanol self-association. Support for the above interpretation is found in the IR spectra in the carbonyl stretching region, shown in Figure 7. In the figure, the carbonyl-stretching band of PBMA is located at 1728 cm^{-1}. There is indication of a shoulder at 1710 cm^{-1} in the spectra of the blends when the silanol composition is between 11 and 33% in the copolymers, i.e., when the silanol block and PBMA reside in the same phase. The shoulder can be seen more clearly by second-derivative analysis and is

Table 3. Glass Transition Temperatures of PS-*b*-PVPDMS-21/PBMA Blends (w/w)

wt % of PBMA	PS T_{g1}[a] (°C)	PVPDMS-21+PBMA T_{g2}[b] (°C)	casting film acetone
0	102	114	clear
16	102	93	clear
33	101	75	clear
50		62 (broad)	clear
67		46 (broad)	clear
84		36 (broad)	clear
100		32	clear

[a] T_{g1} = glass transition temperature of PS. [b] T_{g2} = glass transition temperature of PVPDMS + PBMA phase. The 50, 67, and 84% PBMA films may have different phase relationships.

typical of the hydrogen-bonded carbonyls. On the other hand, the same shoulder is not discernible for blends in which the block copolymers contain higher silanol contents.

In the studies of the miscibility of random copolymers of styrene and 4-vinylphenyldimethylsilanol (poly(styrene-*r*-VPDMS)) and poly(*n*-butyl methacrylate) (PBMA) blends,[4–8] the miscibility windows were located in the composition range of 9−34% VPDMS in the blend films cast from methyl ethyl ketone. In our case, the window for PBMA incorporation into the PVPDMS block is 11−33% VPDMS. The results are comparable. Blends of PBMA with PVPDMS-21 were studied further over a wide range of compositions. The glass transition temperatures of the blends are given in Table 3. The T_g of the PS phase remains at 100 °C when the weight percent PBMA in the blend is 33 or less; at the same time, PBMA is incorporated in the silanol-containing blocks to result in lower T_g's. When the PBMA content reaches 50%, the T_g for the PS domain is no longer detected; only a broad transition appears at a lower temperature. The single broad glass transition may imply morphological changes but requires additional investigation.

PS-*b*-PVPDMS-21/PVPr Blends. Because we have studied in some detail the phase behavior of PS-*b*-PVPDMS-21/PBMA blends, the same block copolymer is selected for blending studies with PVPr, a stronger hydrogen bond acceptor. Figure 8 shows the infrared spectra in the silanol stretching vibration region for PS-*b*-PVPDMS-21/PVPr blends. The infrared spectrum of the block copolymer is characterized by a strong broad band centered at 3429 cm^{-1} (self-association) and a relatively weak band at 3623 cm^{-1} (free) as we have already discussed. For the PS-*b*-PVPDMS-21/PVPr blends, the free silanol absorption band at 3623 cm^{-1} was diminished as the amount of PVPr increased in the blends and disappeared for blends containing more than 50% PVPr. A new band at 3429 cm^{-1} appeared, which was assigned to silanol groups bonded to the amide carbonyls. The location of the peak gradually shifts toward 3429 cm^{-1} as PVPr content increases in the blend. The frequency shift ($\Delta\nu$) between the free silanol band and the silanol−carbonyl stretching band in the blends (206 cm^{-1}) is slightly smaller than the value observed for the self-associated silanols (223 cm^{-1}) of the copolymer itself but substantially larger than the value of 103 cm^{-1} observed in PBMA blends.

The hydrogen-bonding interaction was also revealed in the amide carbonyl-stretching region of the infrared spectra. In Figure 9, the amide carbonyl-stretching band of PVPr occurs at 1662 cm^{-1}. A new strong absorption band at 1643 cm^{-1} appeared upon blending with the

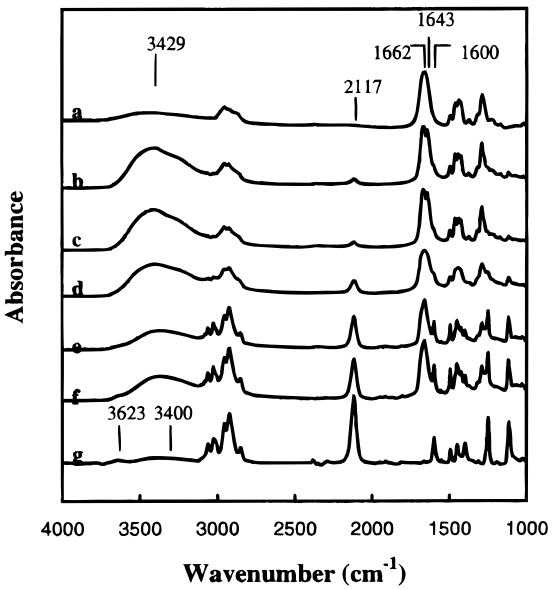

Figure 8. Infrared spectra of PS-*b*-PVPDMS-21/PVPr blends (w/w): (a) PVPr, (b) 16.7%, (c) 33.3%, (d) 50%, (e) 66.7%, (f) 83.3%, and (g) 100% PS-*b*-PVPDMS-21.

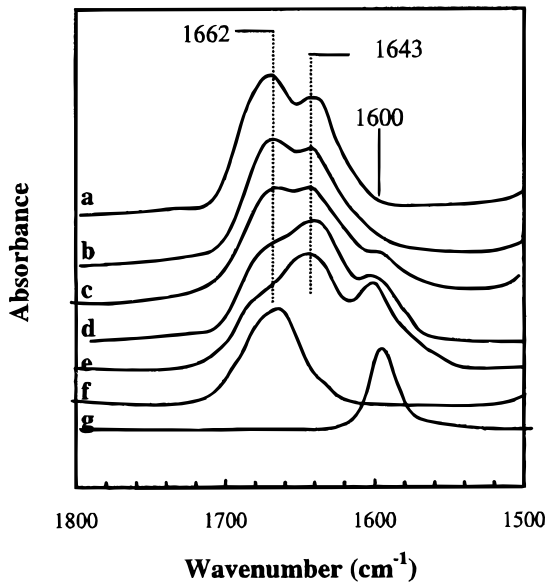

Figure 9. Infrared spectra of carbonyl stretching region in PS-*b*-PVPDMS-21/PVPr blends (w/w): (a) PVPr, (b) 16.7%, (c) 33.3%, (d) 50%, (e) 66.7%, (f) 83.3%, and (g) 100% PS-*b*-PVPDMS-21.

copolymer, which is assigned to the hydrogen-bonded amide carbonyl groups. The absorbance of this band increases with increasing amounts of PS-*b*-PVPDMS-21 in the blends. Two glass transition temperatures were observed for each of the thermal scans of PS-*b*-PVPDMS-21/PVPr blends (Figure 10, top). The transition at 102 °C is obviously the T_g of PS whereas the second T_g, which increases with PVPr content, is due to the silanol-containing phase mixed with PVPr. As a result of strong intermolecular interaction, the T_g of the second phase is higher than the weight-average value, and the data can be fitted by the simplified Kwei equation:[24] $T_g = w_1T_{g1} + w_2Tg_2 + qw_1w_2$. These results, taken together with the clarity of the blend film, are consistent with the mechanism of microphase separation. Note that although PVPDMS-21/PBMA blends containing 16 and 33% PBMA also shows two T_g's,

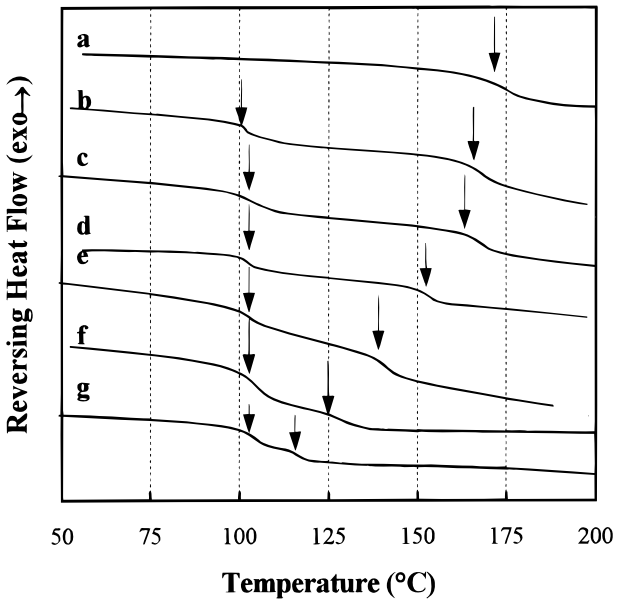

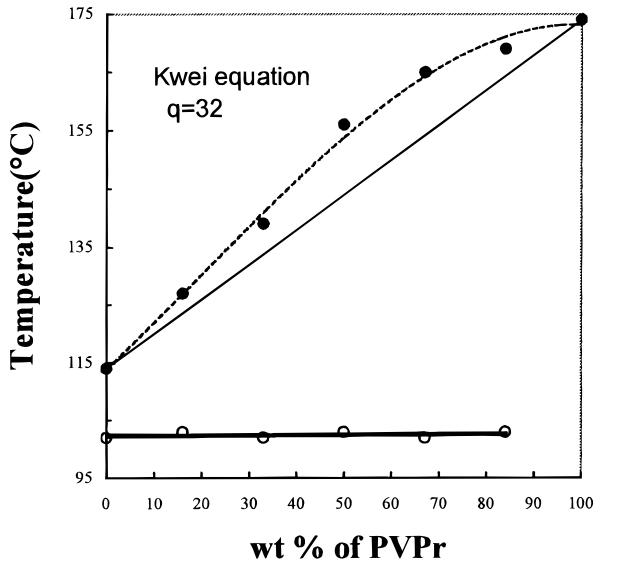

Figure 10. (top) TMDSC curves for PS-*b*-PVPDMS-21/PVPr blends (w/w): (a) PVPr, (b) 16.7%, (c) 33.3%, (d) 50%, (e) 66.7%, (f) 83.3%, and (g) 100% PS-*b*-PVPDMS-21. (bottom) Glass transition temperatures of PS-*b*-PVPDMS-21/PVPr blends as a function of compositions: ○, PS phase; ●, mixed phase of PVPDMS-21 and PVPr.

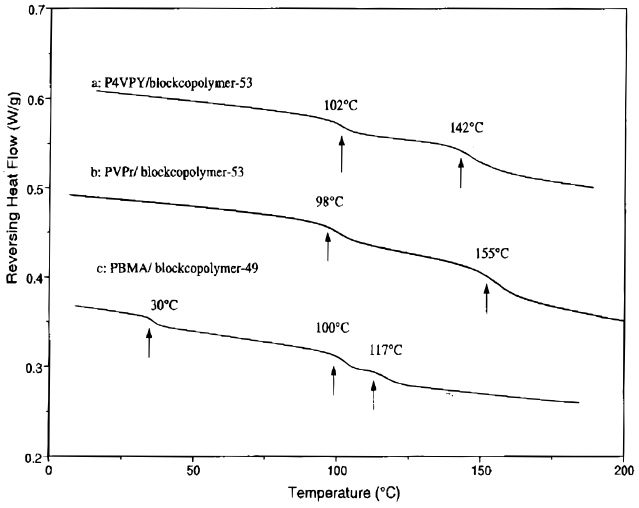

Figure 11. Glass transition temperature of (a) PS-*b*-PVPDMS-53/P4VPy, (b) PS-*b*-PVPDMS-53/PVPr, and (c) PS-*b*-PVPDMS-49/PBMA (50/50) blends PS-*b*-PVPDMS-21/poly(4-vinylpyridine) blends.

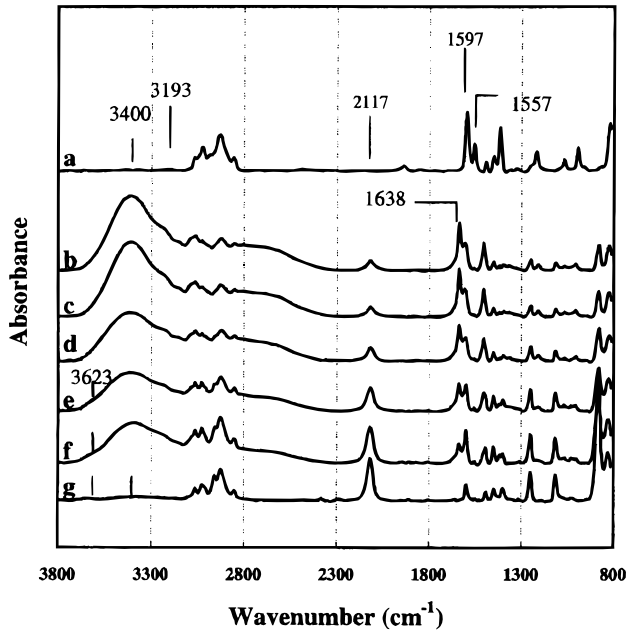

Figure 12. FT-IR spectra of P4VPy/PS-*b*-PVPDMS-21 blends (w/w): (a) P4VPy, (b) 16.7%, (c) 33.3%, (d) 50%, (e) 66.7%, (f) 83.3%, and (g) 100% PS-*b*-PVPDMS-21.

the T_g values of the PVPDMS-21/PBMA microphase are smaller than the corresponding weight-average values because PBMA is a weaker hydrogen bond acceptor bond than PVPr.

The stronger hydrogen-accepting power of PVPr is manifested not only in the synergistic effect on the T_g of the mixed phase but also on the phase relationships in blends of copolymers having high silanol contents. As an example, whereas three T_g's were found for a 50/50 PBMA/PS-*b*-PVPDMS-49 blend (Table 2) indicative of the microphase−macrophase separation mechanism, the PVPr/PS-*b*-PVPDMS-53 blend showed only two T_g's (Figure 11), conforming to the microphase separation mechanism.

PS-*b*-PVPDMS-21/P4VPy Blends. Of the three homopolymers used for the blending studies, P4VPy has the highest basicity. According to Hellmann's analysis, microphase separation should dominate the morphological features. The strong intermolecular interaction is seen readily in FT-IR spectra. Figure 12 shows the FT-IR spectra of the P4VPy blends with copolymer-21. In addition to the free hydroxyl stretching region at 3623 cm^{-1}, a broad band between 3000 and 3700 cm^{-1} represents the absorption of hydroxyl groups that are either self-associated or bonded to the pyridine ring. As the homopolymer content increases, the 3623 cm^{-1} peak weakens and disappears with concomitant increase in the intensity of the 3400 cm^{-1} peak. But unlike the results for the PVPr blends, the position of the 3623 cm^{-1} peak does not change. This suggests that silanol self-association is similar in strength to silanol−pyridine interaction. At the same time, we observe a new band at 3193 cm^{-1} which is thought to result from either overtones and combinations that are intensity enhanced by Fermi resonance[18,19] or inharmonic coupling of the ν_s(O−H stretching) and σ_s(H- -N stretching) modes.[19]

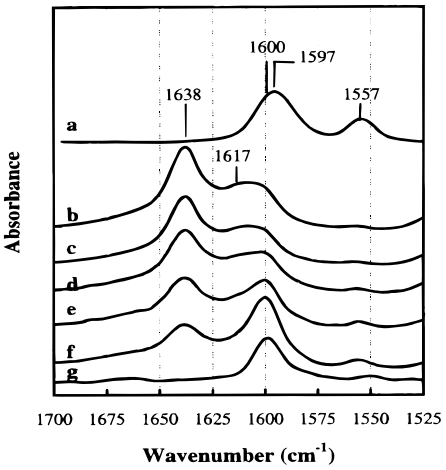

Figure 13. FT-IR spectra in the range 1700−1525 cm^{-1} of P4VPy/PS-*b*-PVPDMS-21 blends (w/w): (a) pure P4VPy, (b) 16.7%, (c) 33.3%, (d) 50%, (e) 66.7%, (f) 83.3%, and (g) 100% PS-*b*-PVPDMS-21.

We also observe a broad band from N−H stretching in the range from 2400 to 2800 cm^{-1}, which indicates proton transfer to the pyridine. Protonation of the pyridine moiety to form pyridinium ring is confirmed by the new peak at 1638 cm^{-1}.[20]

Of the four intense bands corresponding to pyridine ring modes at 1597, 1557, 1415, and 993 cm^{-1}, the 1557 cm^{-1} peak is not affected in position by hydrogen bonding, but the band at 1597 cm^{-1} is (Figure 13). As we increase the copolymer content of the blend to 16.7%, a new shoulder band appeared at 1617 cm^{-1} which can be assigned to the hydrogen-bonded pyridine ring which is to be differentiated from the protonated pyridine. Cesteros et al.[18,21] have observed the same shifts in P4VPy blends with polymer-containing hydroxyl groups. Although the peak is not clearly observed by visual inspection, the second-derivative plot reveals its presence unequivocally. In fact, the two peaks in the 1600−1650 cm^{-1} region at 1638 and 1617 cm^{-1} can be assigned respectively to the stretching bands of the pyridinium ring and hydrogen-bonded pyridine ring (absorption at 1600 cm^{-1} is due to 1, 4-disubstituted benzyl ring of PS-*b*-VPDMS-21). Additional evidence for the hydrogen-bonded pyridine species was provided by the shifts of the 1415 cm^{-1} stretching band of P4VPy by approximately 5 cm^{-1} to 1420 cm^{-1} and of the 993 cm^{-1} band to 1006 cm^{-1}, in agreement with the literature.[22,23] We conclude from the above that silanol−pyridine interaction results in two pyridine species, one being hydrogen bonded in the conventional sense and the other involving proton transfer to form the pyridinium ring.

The glass transition temperatures of the P4VPy blends are listed in Figure 14. For each blend, two T_g's were observed, one being that of the PS domain and the other that of the mixed phase of the homopolymer and silanol-containing block, which increases with homopolymer content. The results are again typical of microphase separation and are consistent with the transparency of the blend films. We have also noticed that the T_g values of the mixed phase can be fitted by the Kwei equation with a q value of 42 (Figure 14), which is to be compared with the value 100−120 obtained from a related blend in which the block copolymer is PS-*b*-poly(*p*-hydroxystyrene). In an additional experiment similar to the one carried out with PVPr, the 50/50 P4VPy/PB-*b*-PVPDMS-53 blend also exhibited only two glass transitions (Figure 11).

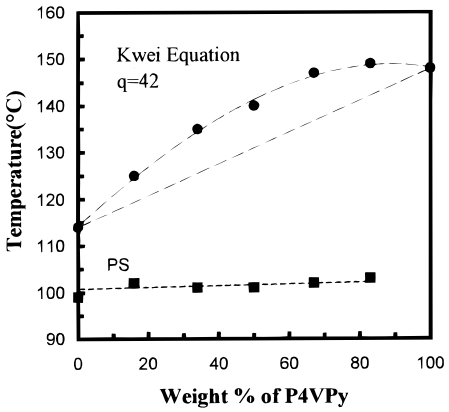

Figure 14. Glass transitions temperatures of P4VPy/PS-*b*-PVPDMS-21 blends as a function of composition: ■, PS phase; ●, mixed phase of PVPDMS-21 and P4VPy.

Conclusions

The results of infrared spectroscopy and glass transition temperature measurements of blends of three different homopolymers with PS-*b*-PVPDMS can be summarized as follows.

(1) The phase relationship in blends of PBMA and PS-*b*-PVPDMS is consistent with morphology development via the microphase separation mechanism when the silanol content of the PVPDMS block is between 11 and 33%. At higher silanol contents, the T_g results that indicate three different domains are indicative of a microphase−macrophase separation mechanism. The underlying reason for this observation is the strong tendency for silanol groups to undergo self-association in the competition with silanol−PBMA interaction.

(2) When the block copolymer is blended with PVPr, a stronger hydrogen bond acceptor than PBMA as evidenced by IR frequency shifts, the T_g results conform to the prediction of a microphase separation mechanism. The T_g of the mixed phase of PVPr and PVPDMS is higher than the calculated weight-average value.

(3) The interaction between the pyridine ring and the silanol group is the strongest of the three homopolymer used. Microphase separation is the dominant mechanism in the morphology development, and there is a large synergistic enhancement of the T_g of the mixed phase due to strong intermolecular interaction.

References and Notes

(1) Lowenhaupt, B.; Steurer, A.; Hellmann, G. P. *Macromolecules* **1994**, *27*, 908.
(2) Zhao, J. Q.; Pearce, E. M.; Kwei, T. K. *Macromolecules* **1997**, *30*, 7119.
(3) Lu, S.; Pearce, Eli, M.; Kwei, T. K. *Macromolecules* **1993**, *26*, 3514.
(4) Lu, S.; Pearce, E. M.; Kwei, T. K. *J. Macromol. Sci., Pure Appl. Chem*. **1994**, *A31*, 1535.
(5) Lu, S.; Pearce, E. M.; Kwei, T. K. *J. Polym. Sci., Polym. Chem. Ed*. **1994**, *32*, 2597.
(6) Lu, S.; Pearce, E. M.; Kwei, T. K. *J. Polym. Sci., Polym. Chem. Ed*. **1994**, *32*, 2607.
(7) Lu, S.; Pearce, E. M.; Kwei, T. K. *Polymer* **1995**, *36*, 2435.
(8) Lu, S.; Pearce, E. M.; Kwei, T. K. *J. Polym. Eng. Sci*. **1995**, *35*, 1113.
(9) Perrin, D. D.; Armarego, W. L. F. *Purification of Laboratory Chemicals*, 3rd ed.; Pergamon Press: New York, 1988.
(10) Grever, G.; Reese, E. *Makromol. Chem*. **1959**, *77*, 13.
(11) Hirao, A.; Hatayama, T.; Nakahama, S. *Macromolecules* **1987**, *20*, 1505.

(12) Ozaki, H.; Hirao, A.; Nakahama, S. *Macromolecules* **1992**, *25*, 1391.
(13) Coleman, M. M.; Graf, J. F.; Painter, P. C. *Specific Interactions and the Miscibility of Polymer Blends*; Technomic: Lancaster, PA, 1991.
(14) Hirao, A.; Gawana, T.; Hatayama, K.; Nakahama, S. *Macromolecules* **1987**, *20*, 242.
(15) Gilman, H.; Smart, G. N. R. *J. Org. Chem*. **1950**, *15*, 720.
(16) Soga, I.; Granick, S. *Macromolecules* **1998**, *31*, 5450.
(17) Ruokolainen, J.; Tanner, J.; Ikkala, O. *Macromolecules* **1998**, *31*, 3532.
(18) Cesteros, L. C.; Isasi, J. R.; Katime, I. *Macromolecules* **1993**, *26*, 7256.
(19) Lee, J. Y.; Painter, P. C.; Coleman, M. M. *Macromolecules* **1988**, *21*, 954.
(20) (a) Sakurai, K.; Douglas, E. P.; Macknight, W. J. *Macromolecules* **1992**, *25*, 4506. (b) Dai, Y. K.; Chu, Evan, Y.; Xu, E. S.; Pearce, E. M.; Okamoto, Y.; Kwei, T. K. *J. Polym. Sci., Part A: Polym. Chem*. **1994**, *32*, 397. (c) Ikkala, O.; Ruokolainen, J.; Brinke, G. *Macromolecules* **1995**, *28*, 7088.
(21) Velada, J. L.; Cesteros, L. C.; Meaurio, E.; Katime, I. *Polymer* **1995**, *36*, 2765.
(22) Takahashi, H.; Mamola, K.; Plyler, E. K. *J. Mol. Spectrosc.* **1996**, *21*, 217.
(23) Ruokolainen, J.; Brinke, G.; Ikkala, O. *Macromolecules* **1996**, *29*, 3409.
(24) Kwei, T. K. *J. Polym. Sci. Lett. Ed*. **1984**, *22*, 307.
(25) French, R. N.; Walsh, J. M.; Machado, J. M. *Polym. Eng. Sci*. **1994**, *34*, 42.
(26) Lu, S. Ph.D. Dissertation, Polytechnic University, Brooklyn, NY, 1996**.**
(27) Chang, H. P. Ph.D. Dissertation, Polytechnic University, Brooklyn, NY, 1996.

MA990852N